OPEN ACCESS

University of BRISTOL

Mandolini, A., Diambra, A., & Ibraim, E. (2016). Evolution of small strain stiffness of granular soils with a large number of small loading cycles in the 3-D multiaxial stress space. In 1st IMEKO TC4 International Workshop on Metrology for Geotechnics, MetroGeotechnics 2016: Proceedings of a meeting held 17-18 March 2016, Benevento, Italy.. (pp. 175-180). IMEKO-International Measurement Federation Secretariat.

Peer reviewed version

Link to publication record in Explore Bristol Research
PDF-document

University of Bristol - Explore Bristol Research
General rights

Evolution of small strain stiffness of granular soils with a large number of small loading cycles in the 3-D multiaxial stress space

Alessandro Mandolini[1], Andrea Diambra, Erdin Ibraim

[1] Department of Civil Engineering, University of Bristol, Bristol, UK
E-mail: am1873@bristol.co.uk

Abstract – **The effect of the application of a large number of small loading cycles on the small strain stiffness of granular soils has been explored in the generalised multiaxial stress space using the Hollow Cylinder Torsional Apparatus (*HCTA*). The experimental investigation has been carried out on an angular to sub-angular silica sand. The sequence of cyclic loading has been performed for a range of stress levels and orientation of the principal stress axes. Accurate measurements of the quasi-elastic properties of the material were obtained using six non-contact displacement transducer (based on eddy current effect) with a resolution of 0.1 μm. Vertical, circumferential and radial strains of the sample could be accurately measured to obtain accurate estimation of Young and Shear moduli at very small strain levels. Changes in both moduli under a sequence of both axial and torque loading cycles will be presented for different initial multiaxial stress conditions.**

I. INTRODUCTION

The understanding of the cyclic loading effect is of crucial importance in the design guidance for offshore geotechnical engineering. Structures such as piles, gravity or suction caissons foundations for off-shore wind farms are subjected to tens of millions of loading cycles throughout their design lives and the consequences of such a large amount of cycles on the soil response are still unknown. Soil surrounding such foundations are prone to high-cycle fatigue damage and their properties can potentially change in a long-term prospect.

  The present experimental investigation aims to provide high-quality experimental data simulating the application of a large number of small loading cycles on Hostun sand by using the Hollow Cylinder Torsional Apparatus. The HCTA is particularly suited for the task because of its ability to apply general stress paths including cyclic rotation of the principal stress (or strain) axes. This condition is widely induced in the ground by many types of loads, such as the cyclic loading from waves on the foundation soil for offshore structures [1].

The employed HCTA apparatus is equipped with a complex strain measurement system based on high-resolution non-contact transducers which enables a very accurate assessment of the sand stiffness in the small strain domain. This paper will present results from 4 tests where sets of large number of small loading cycles (up to 16380) have been applied at different stress conditions in the multiaxial stress space.

II. TESTED MATERIALS AND APPARATUS

A. Hostun Sand

Hostun RF (S28) sand is a standard European material for laboratory testing with a high siliceous amount ($SiO_2 > 98\%$) and angular to sub-angular grain shape. Its grain size distribution is shown in Fig. 1 and its physical properties are as follows: mean grain size D_{50}=0.32 mm, coefficient of uniformity Cu=1.70, coefficient of gradation Cg=1.1, specific gravity Gs=2.65 and minimum and maximum void ratios, respectively e_{min}= 0.62 and e_{max}= 1.00.
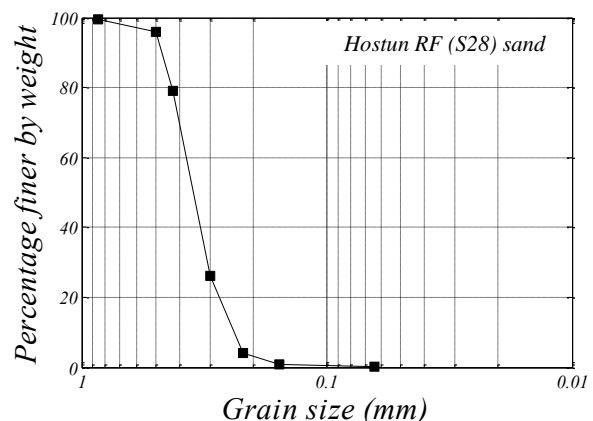

Fig. 1 Grain size distribution, Hostun RF (S28) sand [2].
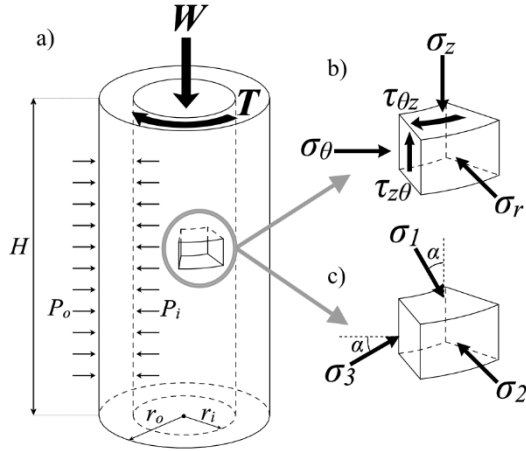
B. Hollow Cylinder Torsional Apparatus

Fig. 2 Stress state in hollow cylinder torsional sample (a). Details of the element in the wall: (b) the stress components and (c) main principal stresses.

The HCTA provides a great freedom to explore general stress and strain soil behaviour and it is particularly suited for the investigation of the mechanical response under cyclic loading conditions. The apparatus has the capability to control axial load (W), torque load (T) and internal and external pressure (Pi and Po) independently (Fig. 2a). The application of these enables the control of all the stress components: axial (σ_z), radial (σ_r), circumferential (σ_θ) and shear stress ($\tau_{\theta z} = \tau_{z\theta}$) on an element of the hollow cylindrical specimen (Fig. 2b). The stress path can be characterized by four independent parameters, such as the mean principal effective stress p' (1), generalised deviatoric component of stress q (2), intermediate principal stress parameter b (3) and the angle α_σ (4) between the major principal stress σ_1 and the vertical direction (Fig. 2c), defined as:

$$p = \frac{\sigma_z + \sigma_\theta + \sigma_r}{3} = \frac{\sigma_1 + \sigma_2 + \sigma_3}{3} \qquad (1)$$

$$q = \sqrt{\frac{(\sigma_z - \sigma_r)^2 + (\sigma_r - \sigma_\theta)^2 + (\sigma_\theta - \sigma_z)^2}{2} + 3\tau_{\theta z}^2} \qquad (2)$$

$$b = \frac{\sigma_2 - \sigma_3}{\sigma_1 - \sigma_3} \qquad (3)$$

$$\alpha_\sigma = \frac{1}{2} tan^{-1} \left(\frac{2\tau_{\theta z}}{\sigma_z - \sigma_\theta} \right) \qquad (4)$$

Soil samples tested in the HCTA have a typical hollow cylindrical shape. The specimens have an outer radius (r_o) of 50mm, inner radius (r_i) of 30mm and 200mm height (H) as shown in Fig. 2a. The geometry helps minimising the degree of stress and strain non-uniformities, inevitable in a hollow cylinder specimen as a result of the sample curvature and the restraint at its ends ([4], [5]).

C. Small Strain Measurament System

A complex system of six high precision non-contact displacement $\mu\varepsilon$ transducers were mounted around the hollow cylindrical specimen. With a resolution of 0.1μm the waterproof transducers represented an accurate tool to measure very small strains (up to 10^{-6}) in three directions. Two pairs of displacement sensors (*S1, S2, S3* and *S4* respectively) aimed towards the axial and circumferential directions to small aluminium targets placed on two metal rings around the specimen (Fig. 3). The rings were horizontal and parallel at the distance of 100mm from each other (*Hc*). They were fixed to the specimen by thin plastic strips glued to the external membrane. Radial strains were evaluated as the difference from radial displacements measured by *S5* and *S6* (Fig. 3). The transducers pointed to aluminium foils which were placed in the internal side of the outer membrane. Variation of the inner radius were difficult to measure directly, instead they were estimated by inner volume changes and vertical displacements of the specimen. Due to the limited measurement range of 2mm each transducer was re-positioned to the offset distance (0.2mm) at the beginning of each shearing stage. Each sensor was intentionally designed to move independently through a complex mounting system which could be manoeuvred from the outside underneath the cell. Preliminary calibration test validated the stability of the output signal from the transducers and assessed the linearity of the measurements.
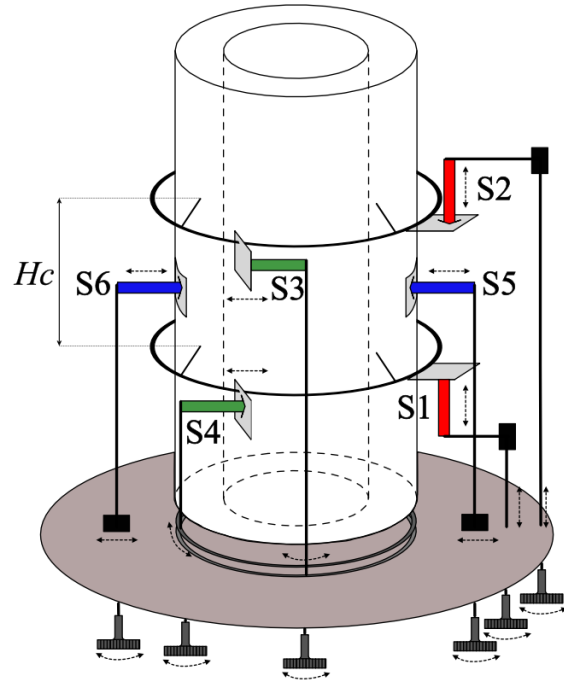

Fig. 3 Schematic view on the small strain measurement system around the hollow cylindrical specimen.

III. SAMPLE PREPARATION

Specimen of sand were reconstituted by dry pluviation followed by vibration. Oven-dried Hostun RF sand was gently poured into the mould through a funnel. The pouring tip was continuously moved up with the surface of the deposit maintaining a constant zero fall height. Once the soil was completely deposited into the mould a dead load was placed on top and vibration was applied. The shaker subjected a vertical vibration to the sample at a frequency of around 55Hz until the target fabrication void ratio of 0.82 was achieved. The samples were tested in fully saturated conditions which were ensured by CO_2 flushing method together with employment of water back pressure up to 300 kPa. Once saturated, the specimen was subjected to an isotropic consolidation performed by manually increasing the cell pressure.

IV. TESTING STRATEGY

A first series of 4 tests were performed at an effective confining pressure of 100kPa held constant during the tests.

Test No.	e_0	$\alpha_{\sigma,m}$	$\alpha_{\sigma,c}$	No. Cycles					
				B	C	D	E	F	G
1	0.819	0º,90º	0º,90º	3240	2880	3240	3240	12240	3240
2	0.816	0º,90º	45º	3240	6480	3780	3420	3330	16380
3	0.825	45º	45º	3780	3240	3240	3240	3240	3420
4	0.838	45º	0º,90º	3240	3240	3240	3240	3240	3240

Table 1 List of the performed tests where ασ,m and ασ,c stand for rotation of the principal stresses during monotonic and cyclic loading respectively and e0 is the initial void ratio.

The testing strategy consisted in imposing a range of deviatoric stress states in the multiaxial stress space and then imposing a large number of deviatoric stress small amplitude cycles (q_{ampl} = ±5kPa) and measuring both Young and Shear moduli at the start and end of each cyclic loading sequence. The four tests are summarised in Table 1 and schematically shown in Fig. 4 in the $\tau_{z\theta}/p'-(\sigma_z-\sigma_\theta)/2p'$ plane. Tests No.1 and No.2 were performed by imposing different level of deviatoric stress states at $\alpha_\sigma=0°$ and 90° (pure compression or extension) as shown in Fig. 4 where the mobilised friction angle (φ'_m) for each deviatoric stress level are also reported. The cyclic sequence was imposed by applying purely compressive/extensive ($\alpha_\sigma=0°$) or torsional ($\alpha_\sigma=45°$) loading cycles respectively for test No.1 and No.2. Tests No.3 and No.4 were instead performed by imposing deviatoric stress state increasing torsional stress only ($\alpha_\sigma=45°$) and them imposing small amplitude stress cycle applying purely compressive/extensive ($\alpha_\sigma=0°$) or torsional ($\alpha_\sigma=45°$) loading cycles respectively.
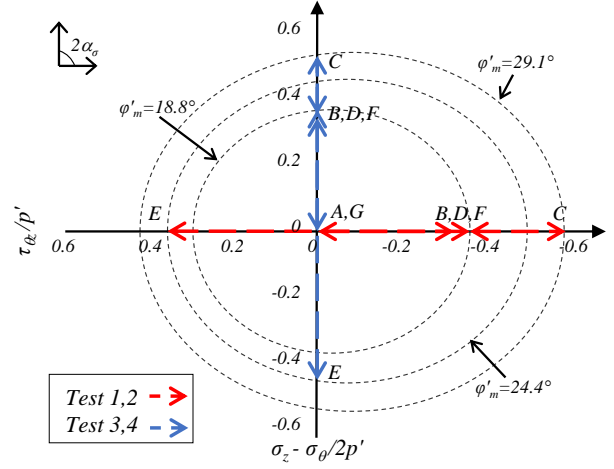

Fig. 4 Imposed stress path in the normalized shear stress-deviatoric stress plane.

Figure 5 reports the time sequence of the stress induced in the sample for Test No.2. The load speed for each monotonic load and unload (blue line in Fig. 5) was kept under 0.5 kPa/min. It is noticeable that when the samples reached the desired deviatoric stress level, creep deformation were allowed to exhaust (green line) before applying the loading sequence. This was necessary to obtain reliable measurements of the elastic small strain stiffness which were not affected by creep deformation.
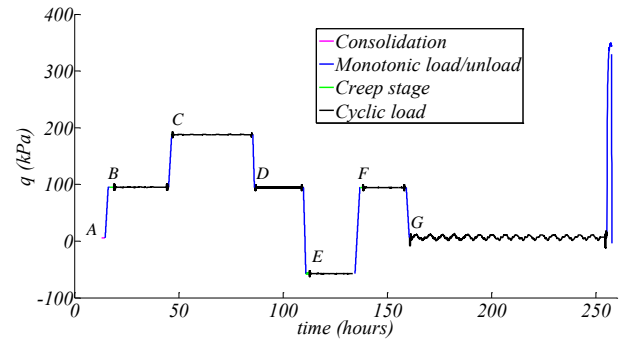

Fig. 5 Evolution of the deviatoric stress (q) for the performed experimental programme.

Then the specimens were subjected to a large number of small loading cycles (black lines in Fig. 5) applied in axial or circumferential direction at the frequency of 0.05Hz which corresponds to a cycle every 20seconds. As shown in Fig. 6, the small strain sample stiffness was measured at investigation points arranged just before and after each cycle, $E_{initial}$ or $G_{initial}$ and E_{final} or G_{final} respectively (Fig. 6).
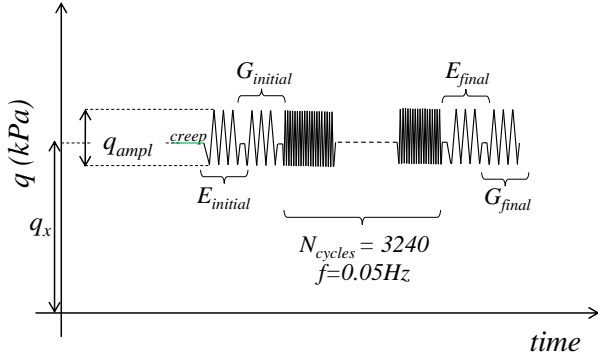
Fig. 6 Schematic representation of cyclic loading procedure applied.

At the investigation points (*ip*) few cycles were applied keeping the same stress amplitude as the main cycle but using a slower frequency (f_{ip}=0.005Hz). This gimmick allowed a detailed data logging and an accurate load control, during which it was possible to estimate both the Young (E_z) and Shear ($G_{θz}$) moduli. Every tests was terminated with a monotonic load to failure in order to assess the strength of the sample (Fig. 5).

V. RESULT AND DISCUSSION

The initial series of test in Table 1 were performed not only to investigate the small strain stiffness on Hostun sand but also in order to assess the response of the transducers and to validate the procedure developed for this experimental experience with the HCTA together with the analysis of the output data. A preliminary analysis showed a first rather definitive output in line with findings from previous experience with the apparatus by [3]: the evaluation of the sample stiffness through external measurement system usually leads to an underestimation of the soil stiffness (Fig. 7).
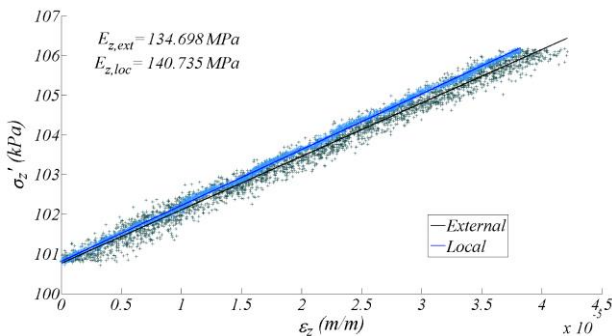

Fig. 7 Young modulus (E_z) measured in triaxial compression and extension: comparison local and external strain measurement systems.

Conventional external measurements of displacement contain systematic errors as result of bedding at the end platens and the effect of compliance in the apparatus [6][7].
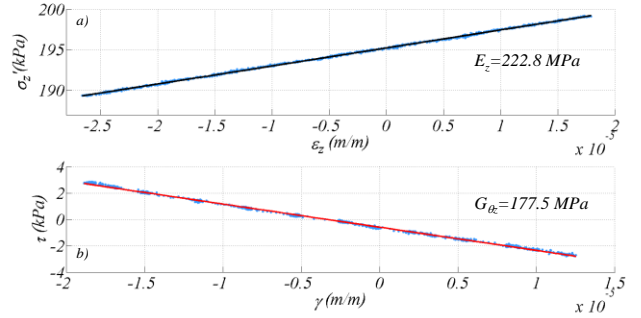

Fig. 8 Stress and strain relationship for a single cycle of q=±5 kPa: in axial direction (a) with relative Elastic (E_z) modulus and in torsional direction (b) with Shear moduli ($G_{θz}$) measured at the ip of test 2.

Internal strain transducer in axial, radial and circumferential direction help to minimise these errors in order to get more realistic soil strains. Young and Shear moduli were evaluated through the slopes of stress and locally measured strain curves (Fig. 8). Previous experimental investigations established the influence of the soil density and the stress conditions on soil stiffness. Fig. 9 aims to extract a relation between the Shear modulus ($G_{θz}$), the specimen void ratio (*e*) and mean principal stresses (*p'*). Based on an extended investigation on Hostun RF sand on the shear wave propagation in triaxial conditions, [8] suggested the void ratio function *f(e)* used to normalise $G_{θz}$ removing the effect of the soil density (Fig. 9). The p'/p_r exponent value of 0.54 resulted within the expected value for sands [3].
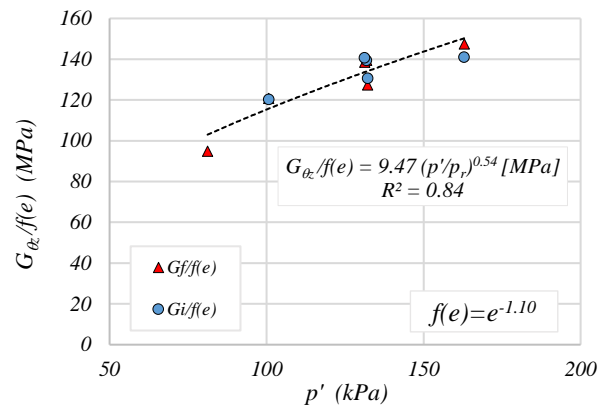

Fig. 9 Shear moduli ($G_{θz}$) compare with mean pressure for test 2 (p_r represents a reference pressure of 1 kPa).

As explained in section IV, in order to detect stiffness variations measurements of both moduli were run at the initial and final *ip* of each stage. Fig. 10 summarises the Shear and Young modulus ratios between the initial and final *ip* (red and black markers respectively) of each stage for all tests. It can be observed that on the range of deviatoric pressure applied the specimens conserved their stiffness after the application of the cyclic loads.
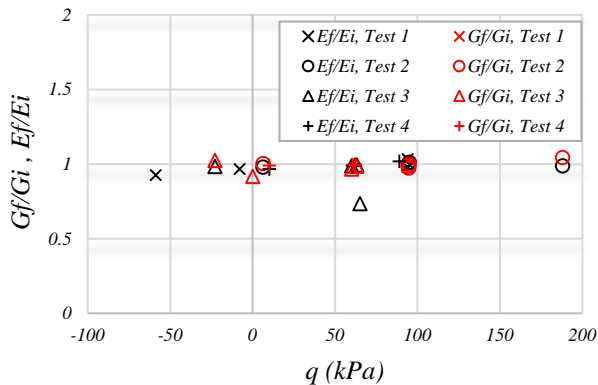
Fig. 10 Elastic (E_z) and Shear moduli ($G_{\theta z}$) ratio between initial and final investigation points (ip) for each test.

Except for one case, the measured small strain stiffness variations were found within 10% from the original values. This suggests that the imposed cyclic loading sequence induced negligible variation of stiffness. While a more accurate analysis of the tests is ongoing, further tests imposing larger number of cycles are also planned.

VI. CONCLUSIONS AND FUTURE INVESTIGATIONS

A new investigation on the small strain stiffness with a Hollow Cylinder Torsional Apparatus is presented. Six high-resolution non-contact displacement transducers provided an accurate measurement of the very small strain of the specimen contributing on the estimation of Young and Shear moduli. Evaluation of the strains through conventional external measurement system contains errors which frequently underestimate the actual soil stiffness of the specimen. The imposed probing stress path described in this paper intends to take the specimen to specific different stress states by using combination of different loading directions with the aim to produce high-level experimental data potentially useful to simulate the conditions of a real case scenario. Despite thousands of small amplitude cycles applied to the specimen the quasi-elastic coefficients, E_z and $G_{\theta z}$, were found to be essentially unchanged before and after the application of the cycles for the whole range of stresses and loading directions imposed in this investigation. Although the experimental campaign is still in its preliminary stage the results obtained encourage both the development of a future testing strategy and many improvements on the data analysis. More drained tests on Hostun sand specimens are surely needed before draw conclusions on the evolution of small strain stiffness anisotropy during cyclic loading. Confinement pressure, cyclic testing conditions, type of loading together with the soil features (density, particle size, and mineralogy) will be the key parameter when planning the next testing programme.

REFERENCES

[1] Arthur, J. Robin F., Chua, Ken S.; Dunstan, Treve, (1980) Principal stress rotation: a missing parameter, American Society of Civil Engineers, Journal of the Geotechnical Engineering Division **106** (4), 419 -433.

[2] Mandolini, A., (2014) Investigation of the strength anisotropy of fibre reinforced sands under generalised condition using the HCTA, Department of Civil Engineering. University of Bristol, p. 132.

[3] Ibraim, E., Christiaens, P., Pope, M., (2011) Development of a hollow cylinder torsional apparatus for pre-failure deformation and large strains behaviour of sand. Geotechnical Engineering Journal of the South-east Asian Geotechnical Society (SEAGS) & Association of Geotechnical Societies in South-East Asia (AGSSEA), Special Issue on Soil Behaviour **42**, 58-68.

[4] Sayão, A. and Vaid, Y.P., (1991) A critical assessment of stress non-uniformities in Hollow Cylinder Test Specimens, Soils and Foundations, Vol. **31**(1), 61-72.

[5] Hight, D.W., Gens, A., Symes, M.J., (1983) The development of a new hollow cylinder apparatus for investigating the effects of principal rotation in soils. Géotechnique **33**(4), 355-383.

[6] Jardine, R. J., Symes, M. J., Burland J. B. (1984) The Measurement of soil stiffness in the triaxial apparatus. Géotechnique **34**(3), 323-340.

[7] Viggiani G. and Atkinson, J. H. (1995) Stiffness of fine-grained soil at very small strains. Géotechnique **45**(2), 249-265.

[8] Escribano, D. (2014) Evolution of stiffness and deformation of Hostun sand under drained cyclic loading. PhD thesis. Department of Civil Engineering. University of Bristol, p. 156.